RSC Advances

ROYAL SOCIETY OF CHEMISTRY

www.rsc.org/advances

A novel magnetic nanocomposite has been successfully synthesized by *in situ* polymerization method using the functionalized Fe_3O_4 nanoparticles as fillers and the hyperbranched waterborne polyurethane (HWPU) as matrix. The results indicated that the introduction of functionalized Fe_3O_4 contributed to thermal stability, the glass transition temperature, hardness and solvent resistance. Furthermore, the nanocomposite films with excellent magnetic properties, which would have a promising application in microwave - absorption field.

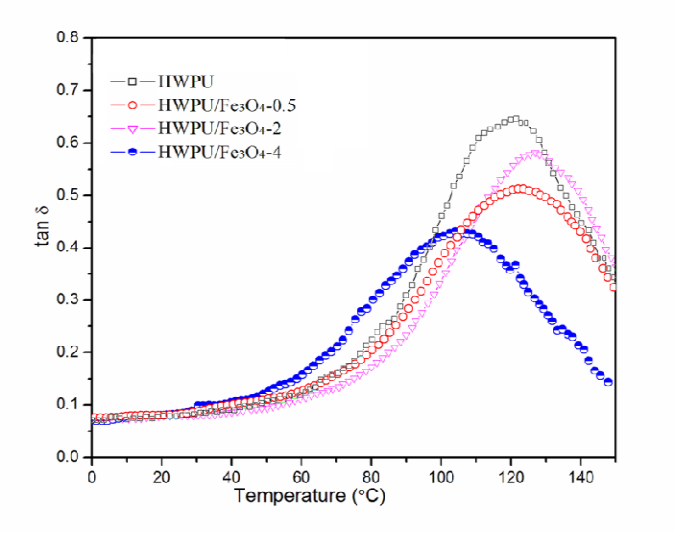

DMA loss factor curves of nanocomposites with different Fe_3O_4-VTEO content.

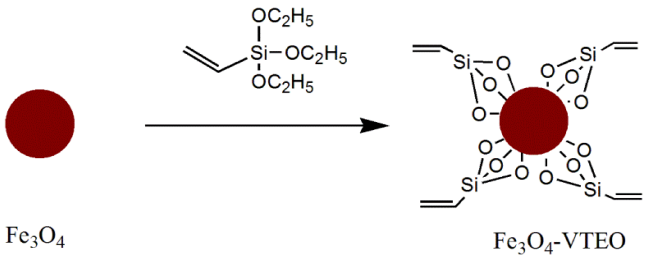

Fig. 1. The reaction scheme of functional Fe_3O_4.

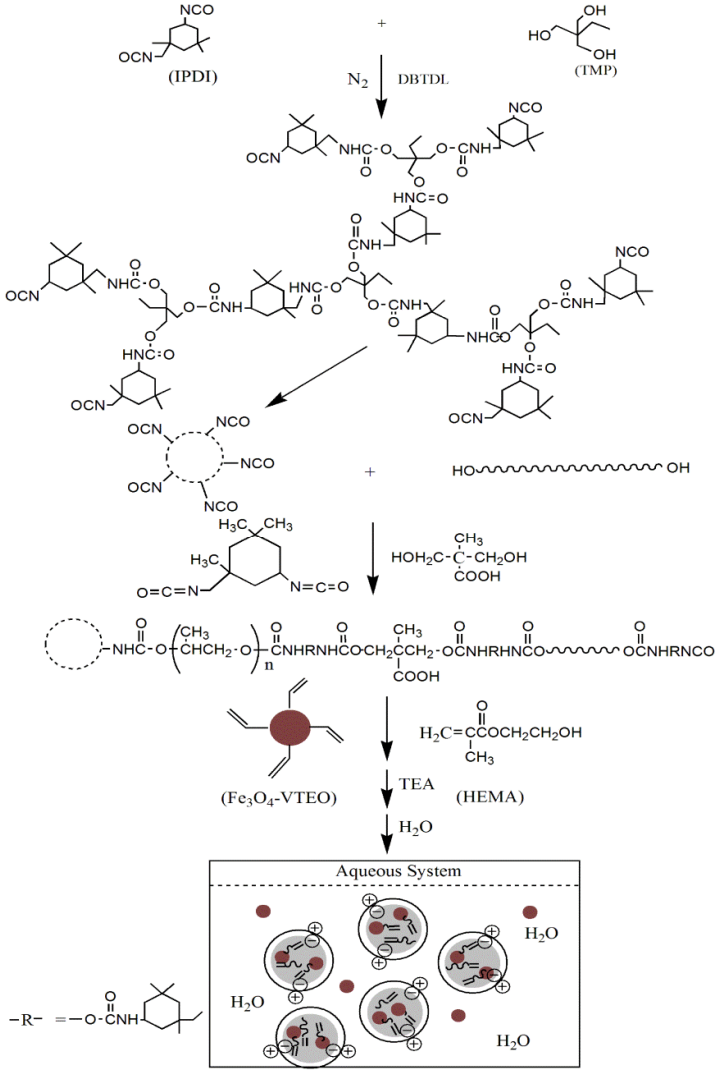

Fig. 2. The flowchart of the preparation of HWPU/Fe_3O_4 nanocomposite emulsion.

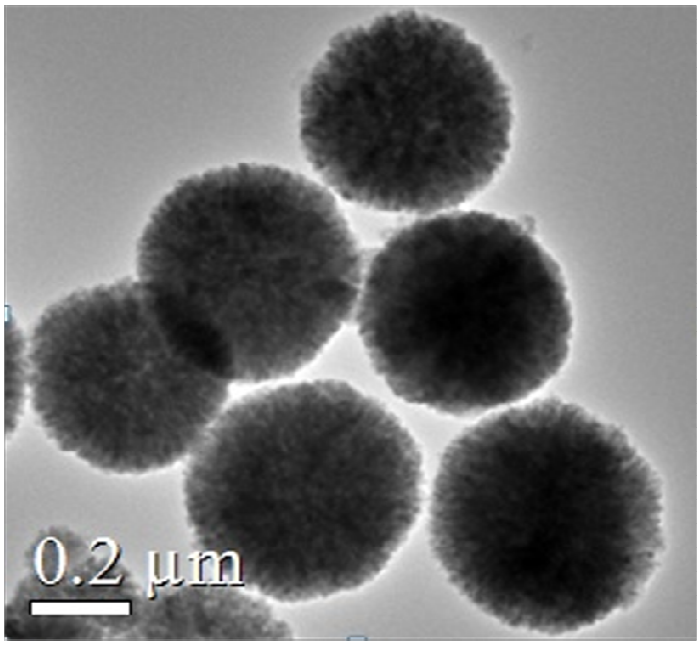

Fig. 3. TEM image of Fe_3O_4 particles.

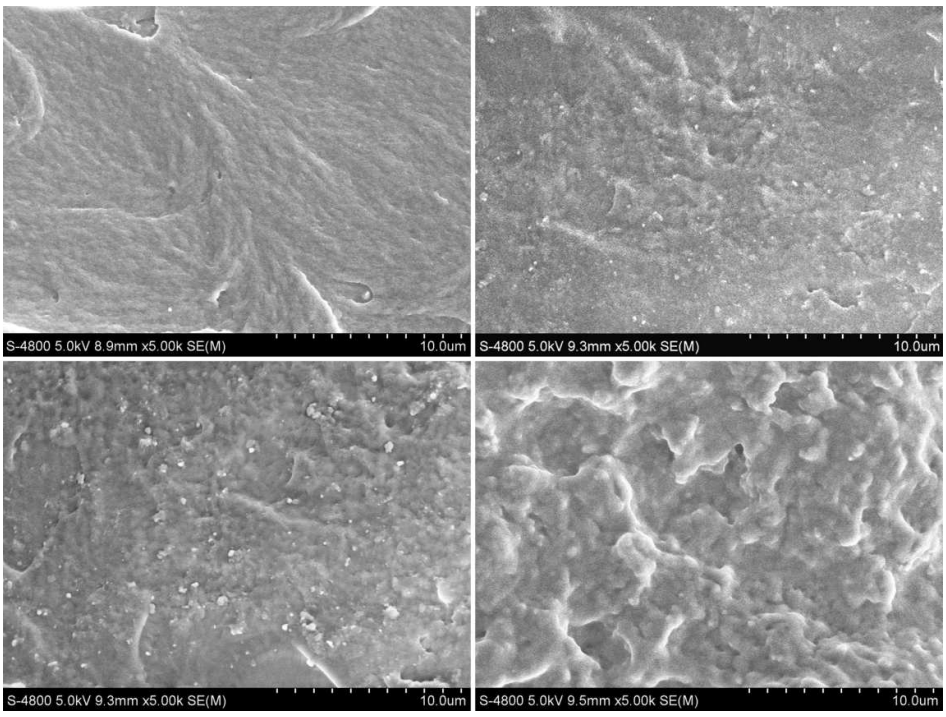

Fig. 4. SEM micrographs of fractured section of pure HWPU (a), HWPU/Fe_3O_4-0.5 (b), HWPU/ Fe_3O_4-2 (c) and HWPU/ Fe_3O_4-6.

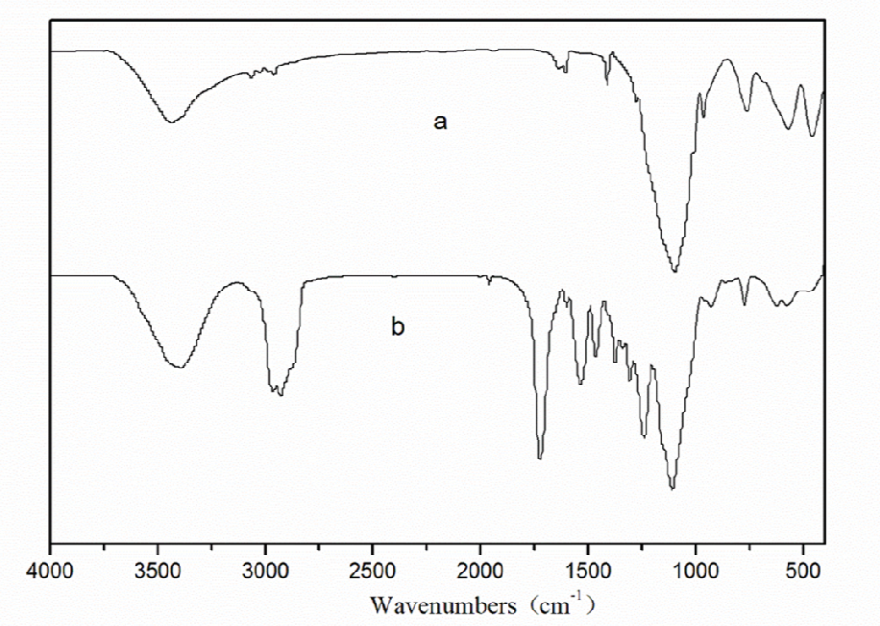

Fig. 5. FT-IR spectra of Fe_3O_4-VTEO (a) and HWPU/Fe_3O_4-2 (b).

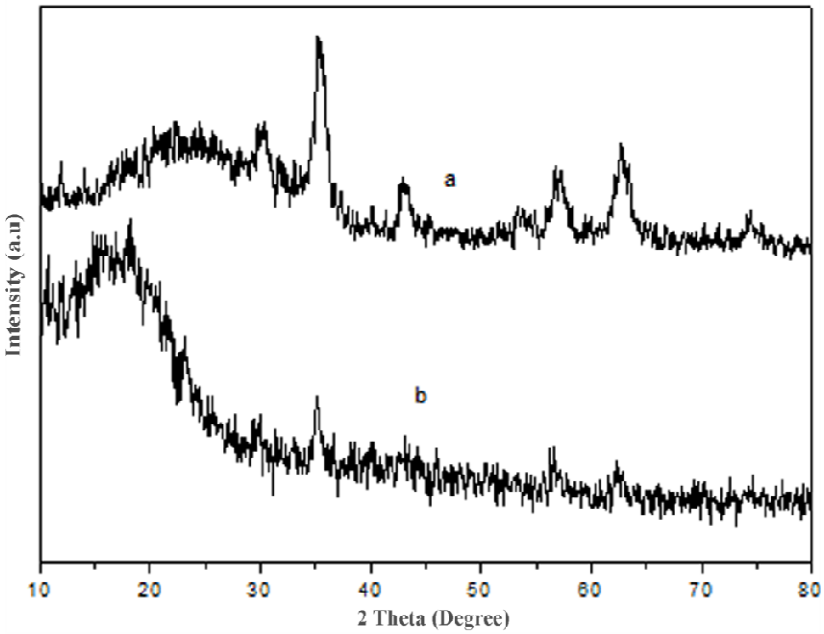

Fig. 6. XRD patterns of Fe_3O_4-VTEO (a) and HWPU/Fe_3O_4-4 (b).

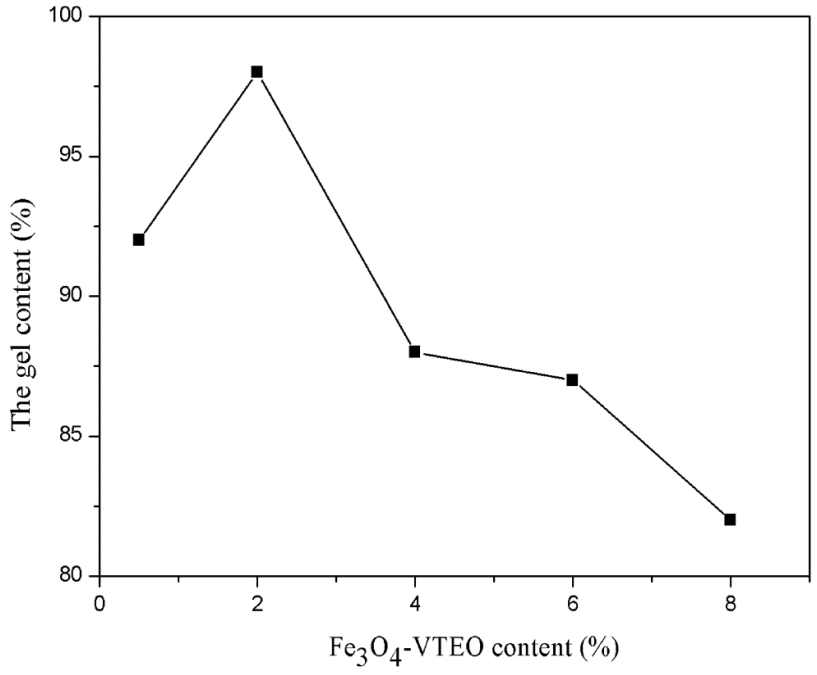

Fig. 7. The gel content of nanocomposites with different Fe_3O_4-VTEO content.

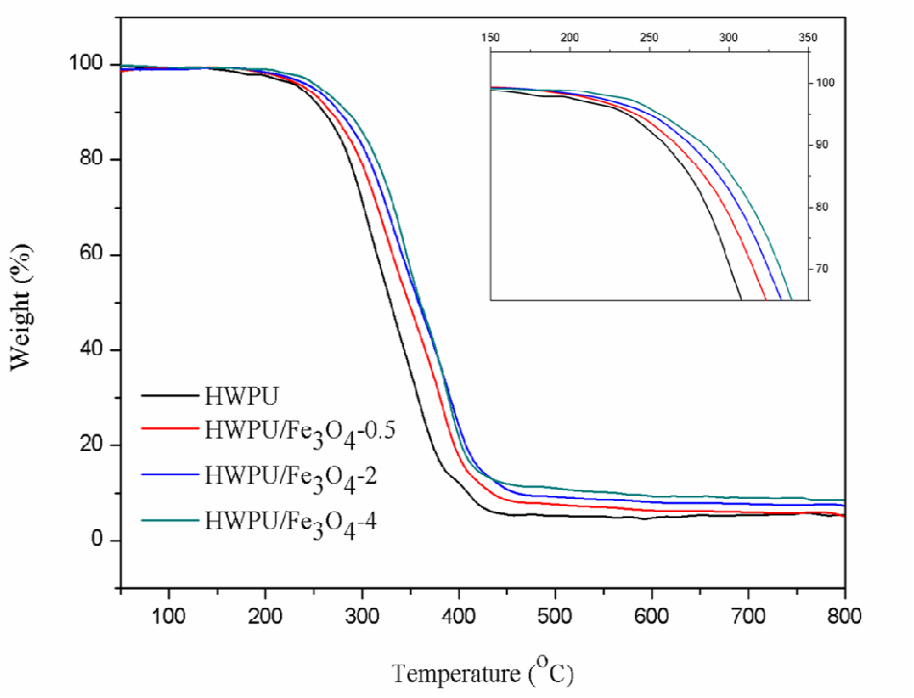

Fig. 8. TGA curves of pure HWPU and HWPU/Fe_3O_4 nanocomposites with different Fe_3O_4-VTEO content.

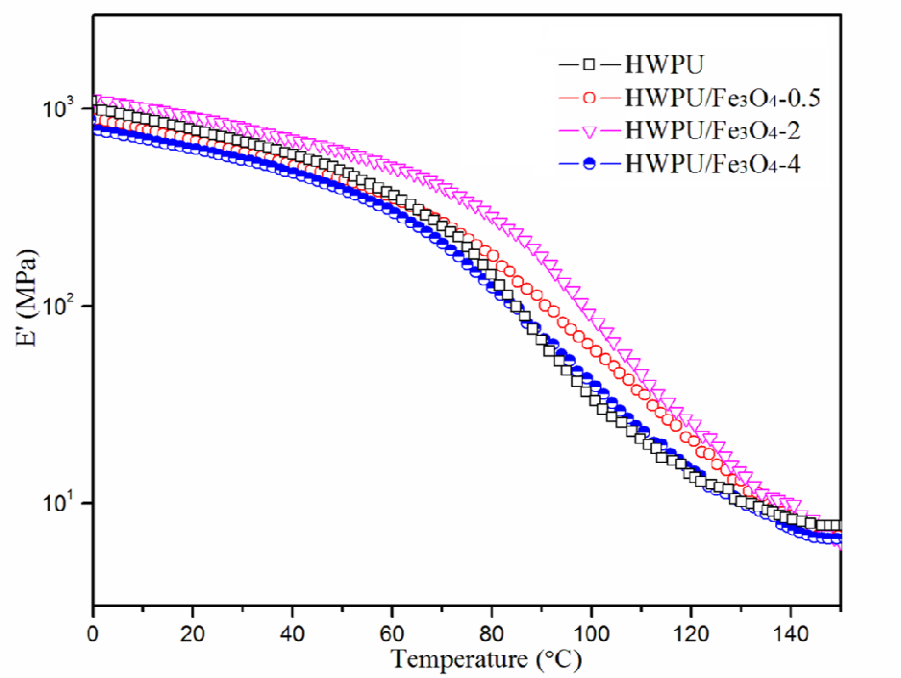

Fig. 9. DMA storage modulus curves of nanocomposites with different Fe_3O_4-VTEO content

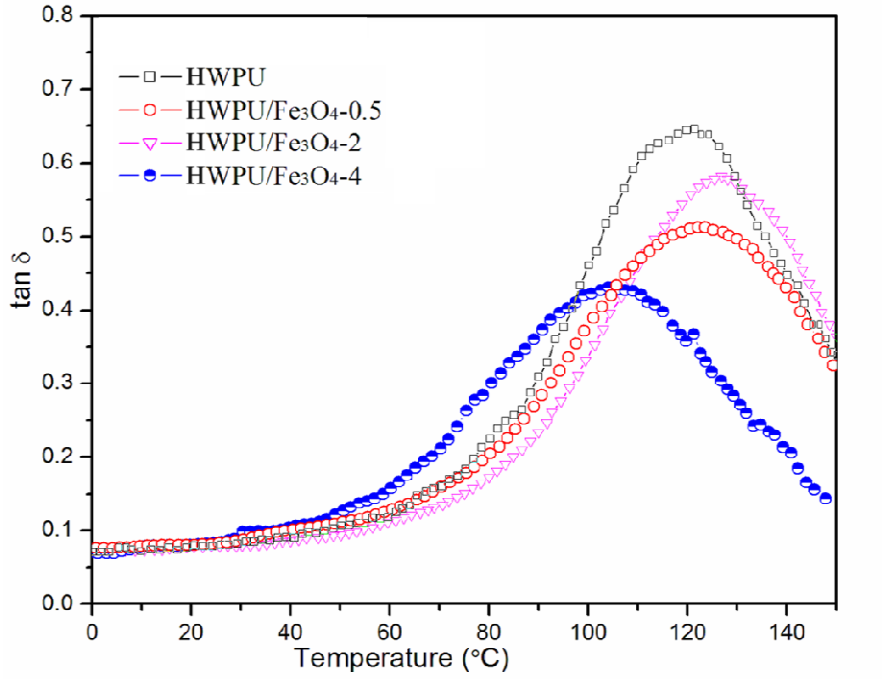

Fig. 10. DMA loss factor curves of nanocomposites with different Fe_3O_4-VTEO content.

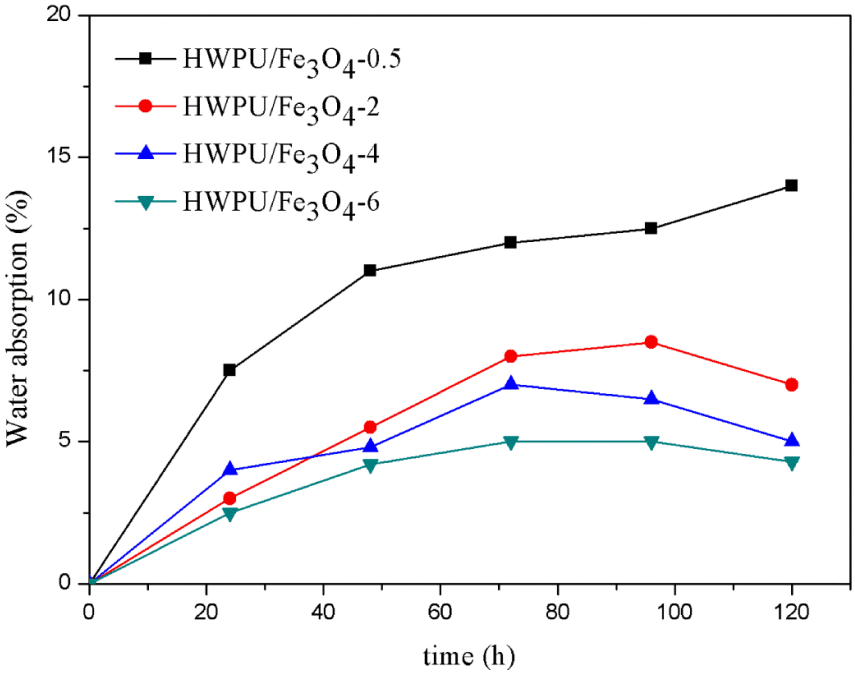

Fig. 11. Influence of Fe_3O_4-VTEO content on water absorption of films.

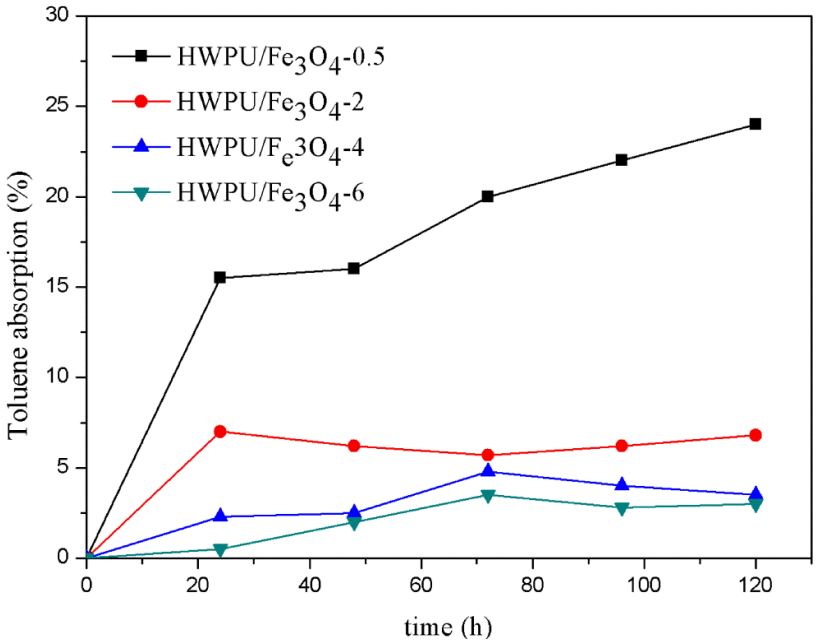

Fig. 12. Influence of Fe_3O_4-VTEO content on toluene absorption of films.

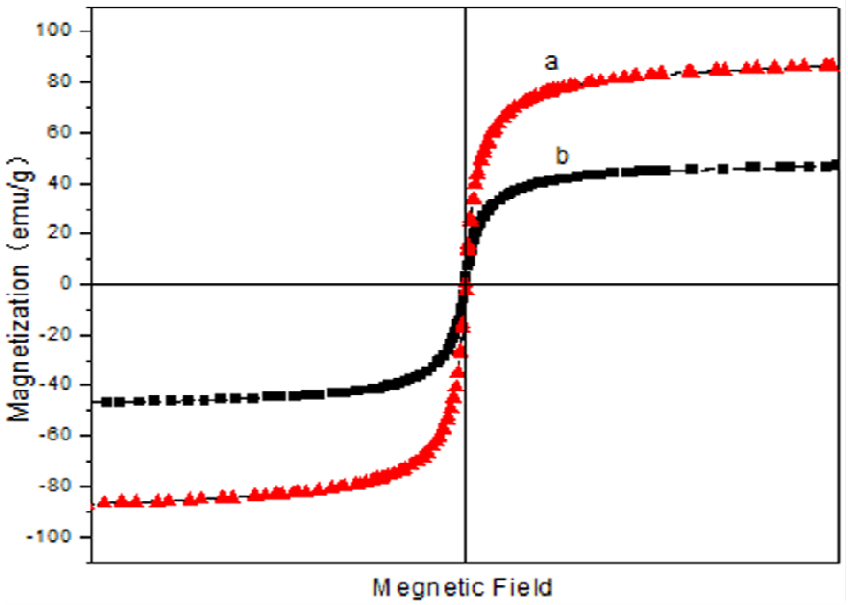

Fig. 13. Hysteresis loops of Fe_3O_4 (a) and Fe_3O_4-VTEO (b).

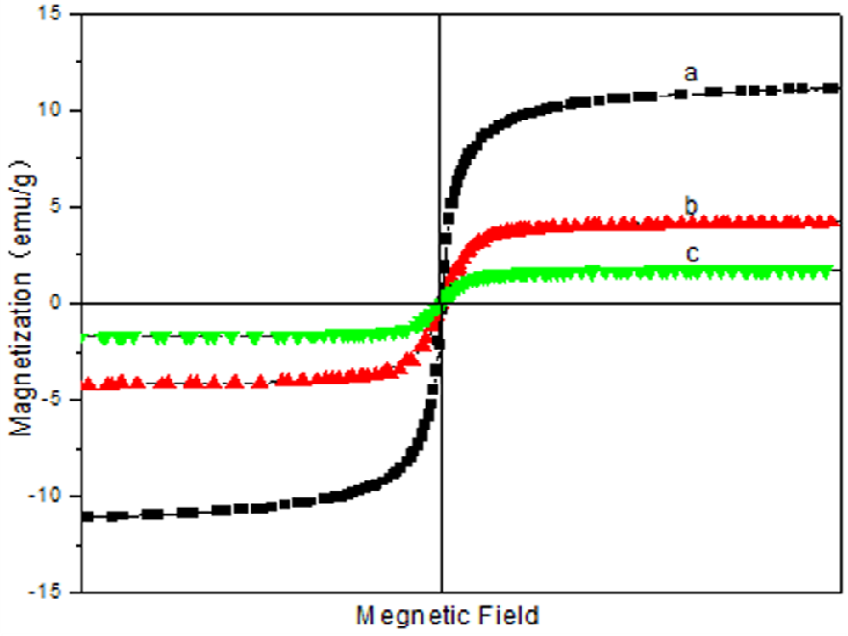

Fig. 14. Hysteresis loops of HWPU/Fe3O_4 nanocomposites with the Fe_3O_4-VTEO content is 8% (a), 4% (b) and 0.5% (c).

Synthesis and properties of novel UV - curable hyperbranched waterborne polyurethane/Fe_3O_4 nanocomposite films with excellent magnetic properties

Suli Chen, Sidi Zhang, Yanfeng Li*, Guanghui Zhao

State Key Laboratory of Applied Organic Chemistry, Key Laboratory of Nonferrous Metal Chemistry and Resources Utilization of Gansu Province, College of Chemistry and Chemical Engineering, Institute of Biochemical Engineering and Environmental Technology, Lanzhou University, Lanzhou, 730000, China

A novel magnetic nanocomposite has been successfully synthesized by *in situ* polymerization method using the functionalized Fe_3O_4 nanoparticles as fillers and the hyperbranched waterborne polyurethane (HWPU) as matrix. The Fe_3O_4 nanoparticles prepared by solvothermal method were modified by vinyltriethoxysilane (VTEO) to improve the compatibility with HWPU, because the functionalized Fe_3O_4 nanoparticles could form effective crosslink points and combined with the HWPU by covalent bonds during the UV-curing process. The microstructure, morphology, emulsion stability, thermal behavior, gel content, mechanical properties, water resistance, solvent resistance and magnetic properties of nanocomposites have been characterized and investigated. It was found that the introduction of functionalized Fe_3O_4 contributed to the thermal stability, glass transition temperature, hardness and solvent resistance of the nanocomposites. What's more, the HWPU/ Fe_3O_4 displayed excellent magnetic behavior, which would have a promising application in microwave - absorbing field.

1. Introduction

Recently, a lot of research has been focused on nanocomposites system in many fields. In particular, inorganic - polymer nanocomposites have drawn great attention

* Corresponding author. Fax: 86-931-8912113; E-mail : liyf@lzu.edu.cn (Yanfeng Li)

due to some advantages that the nanocomposites possessed, such as high stability, superior mechanical properties, excellent electrical, magnetic properties etc. [1, 2] In this context, inorganic particles usually acted as fillers in different polymer matrix and the results indicated that performances of resulting materials were enhanced. Generally, metal particles like Au and Ag, [3, 4] oxides like SiO_2, Al_2O_3, Fe_2O_3, TiO_2 etc., [5-9] carbon material like graphene oxide, carbon nanotube and carbon black, [10-14] silicates like attapulgite, montmorillonite, kaoline, [15-17] etc. have been added in polymer matrix.

Waterborne polyurethane (WPU) is a new type of polyurethane system, namely the polyurethane is dispersed in water rather than in organic solvents. Compared with the conventional polyurethane (PU), waterborne polyurethane exhibits the attractive characteristics of low viscosity, high molecular weight, environment friendly, competitive price, etc. [18, 19] Therefore waterborne polyurethane has potential application and has become a kind of burgeoning and active branch of polyurethane chemistry and technology. However, because of linear structure of most WPUs, the pure WPU frequently presents poor mechanical properties, low thermal stability and water, solvent resistance, which blocked the development and application of WPU. Some measures have been taken to improve properties of WPU, for example, adding inorganic particles, increasing crosslink of density etc. In previous works, kinds of inorganic particles have been added to WPU matrix, such as SiO_2, [20] MWCNTs, [21] Fe_3O_4, [22] Ag, [23] etc. However, in most reported works, WPU nanocomposites have been obtained by simple mechanical mixing and the inorganic nanoparticle tended to aggregate of itself, which has a negative effect on properties of nanocomposites. Furthermore, inorganic particles usually only used to enhance the properties of WPU without other functional. [24-26]

Fe_3O_4 particle is a common form of magnetic ferrite that with cubic inverse spinel

structure. [27] Fe_3O_4 has become the most common and recognized modification material of polymer due to the nanometer effect, strong inorganic rigidity and high saturation magnetization. To the best of our knowledge, using Fe_3O_4 as filler in WPU system to investigate the physical properties and magnetic properties of composites has not drawn much attention today, which is mainly due to the poor stability of nanocomposite emulsion. Compared with other inorganic nanoparticles, Fe_3O_4 particles have bigger density and serious aggregation. The Fe_3O_4 particles would easily settle from the composite system before film formation unless strong interaction was formed between the Fe_3O_4 particles and WPU chains, which made it difficult to obtain final nanocomposites. Adding Fe_3O_4 in WPU matrix not only makes up for the defects of WPU but also endows polymer with magnetic properties. Therefore, this kind of nanocomposite material will be hopefully applied in various fields, especially polyurethane as coating in the microwave - absorbing field. [28] The nanocomposites can be coated on aircrafts and ships surface to reduce the sensitivity of the radar, and also widely used in anechoic chambers, [28] etc. Nonetheless, the Fe_3O_4 particles easily aggregate due to the small size, larger specific surface area and rich in hydroxyl of Fe_3O_4 surface, thereby this may make Fe_3O_4 particles can't be dispersed in WPU matrix in nanoscale, which would greatly affect the performance of the resulting nanocomposites.

In this study, a series of WPU/Fe_3O_4 magnetic nanocomposites have been prepared by *in situ* polymerization method. Trimethylolpropane (TMP) was added to form a hyperbranched monomer firstly to further improve crosslink density of WPU. The Fe_3O_4 nanoparticles used as fillers were modified by vinyltriethoxysilane to prevent agglomeration and increase the compatibility with HWPU matrix. The functionalized Fe_3O_4 contained plenty of C=C double bonds which can crosslink with C=C double

bonds in HWPU chains in the UV curing process. Fe_3O_4 will combine with WPU through chemical bonds. Moreover, functionalized Fe_3O_4 acted as an effective crosslink point, which would contribute to better physical properties of nanocomposites. The microstructure, morphology, thermal behavior, mechanical properties, magnetic properties etc. are characterized by TEM, SEM, XRD, FT-IR, DMTA, tensile testing, VSM, respectively.

2. Experimental

2.1. Materials

Ferric chloride hexahydrate ($FeCl_3 \cdot 6H_2O$), triethylamine (TEA) and dibutyltin diaurate (DBTDL) as catalyst were purchased from Tianjin Chemical Reagent Factory one (China). Poly (propylene glycol) (PPG-2000) and trimethylolpropane (TMP) were obtained from Sinopharm Chemical Reagent Co., Ltd (China). Isophorone diisocyanate (IPDI) was purchased from Shanghai Chemical Reagents Corp. (China). Dimethylol propionic acid (DMPA) was obtained from Aldrich Chemical (China). Vinyltriethoxysilane (VTEO) was purchased from Wuhan University Silicone New Material Co. Ltd (China). Ethylene glycol (EG) and sodium acetate (NaAc) were supplied by Tianjin Chemical Reagent Factory two (China). Irgacure 2959 as photoinitiator was obtained from Sigma-Aldrich Co. TEA, toluene, and acetone were dehydrated via 4Å MS before use. DMPA and TMP were dried in vacuum at 80 °C for 24 h. All other chemicals and reagents were of analytical grade and used as received.

2.2. Synthesis and chemical modification of Fe_3O_4 particles.

The Fe_3O_4 particles were prepared by typical solvothermal method according to the published literature. [29] As follows: 0.9730 g of $FeCl_3 \cdot 6H_2O$ and 1.9460 g of NaAc were dissolved in 30 mL ethylene glycol in a dry flask under mechanical stiring and ultrasonic. The obtained homogeneous solution was transferred to a Teflon-lined

autoclave (100 mL) and sealed to heat at 200 °C for 12 h. After cooling to room temperature, washing the black magnetic product with ethanol and distilled water in sequence by magnetic decantation. The Fe_3O_4 was dried in vacuum at 40 °C for 24 h. Subsequently, the prepared Fe_3O_4 particles were chemically modified by vinyltriethoxysilane (VTEO) as follows: 2.00 g of Fe_3O_4 particles and the same amount of ethanol mixed with water were added into in a flask equipped with a mechanical stirrer, followed by the addition of 8 mL VTEO with constant stirring for 24 h at ambient temperature. The final product was washed with ethanol for times and dried in vacuum at 30 °C for 12 h. The process was shown in Fig. 1.

2.3. Preparation of HWPU/ Fe_3O_4 nanocomposite emulsion

In a three-necked flask equipped with a condenser, mechanical stirrer and a nitrogen (N_2) inlet, a calculated amount of IPDI and 5~6 drops of DBTDL were added. The system was slowly heated up, followed by addition of quantitative TMP dissolved in acetone to the mixture when the temperature reached to 60 °C and reacted for 30 min. Quantitative PPG-2000 and IPDI were added and heated up to 80 °C, allowing react for 2 h. The DMPA was introduced and reacted for another 2 h. It was necessary to add acetone to adjust the system viscousity during above process. Subsequently, the system was cooled to 60 °C and added certain amount of HEMA and Fe_3O_4-VTEO, cooling to 40 °C after reacting for 3 h. The mixture was neutralized by TEA and stirred for 30 min at 40 °C. Lastly, a certain amount of distill water was added to emulsify to obtain final HWPU/Fe_3O_4 emulsion with the solid content was 40%. The synthesis scheme of nanocomposite emulsion was shown in Fig. 2. The HWPU was

prepared according to following molar ratio: IPDI/PPG/DMPA/TMP/TEA= 3.5/1.0/1.0/1.5/1.0.

2.4. The film preparation

The latex films were prepared by mixing reweighted above emulsion with 3wt.% Irgacure 2959 in a flask to form a homogenous dispersion. Spreading the dispersion on a clean Teflon plate surface and placing for 8 h at room temperature to remove most of water before curing. Finally, the latex films were obtained by exposing the samples under ultraviolet light to cure for 4 min. the UV lamp used here was medium-pressure mercury lamp with the power and wavelength of 1000 W and 295 nm, respectively. The distance between UV light and surface of film is 40 cm. Additionally, the final nanocomposite films prepared in this paper with Fe_3O_4-VTEO content of 0, 0.5, 2, 4 and 6wt.% were coded as HWPU, HWPU/ Fe_3O_4-0.5, HWPU/ Fe_3O_4-2, HWPU/ Fe_3O_4-4 and HWPU/ Fe_3O_4-6, respectively, and the rest by analogy.

2.5. Characterization

Power X-ray diffraction (XRD, Rigaku D/MAX-2400 X-ray diffractometer with Ni-filtered Cu Kα radiation) was used to investigate the crystal structure of Fe_3O_4 nanoparticles. The microstructure and morphology of Fe_3O_4 nanoparticles were characterized by transmission electron microscopy (TEM, FEI Tecnai G20). The morphology of film products were investigated using scanning electron microscopy (SEM, JSM-6380Lv, JEOL, Japan; JSM-6701F, JEOL, Japan). FT-IR spectra were conducted on a Fourier-transform infrared spectrophotometer (American Nicolet Corp. Model 170-SX). The thermal gravity analysis (TGA)

curves were obtained from TA Instrument (NETZSCH STA 449C) with the temperature ranging from room temperature to 800 °C. Dynamic mechanical thermal analysis (DMA, Mettler-Toledo) was performed from -30 to 200 °C at the heating rate of 3 °C min^{-1}, the size of sample was 9 mm × 4 mm (0.4 mm thick). The mechanical properties of films are measured by drawing machine (Instron1122) according to the national standard GBI447-83 with the drawing speed of 30 mm/min. The hardness of nanocomposite films is measured by QHQ hardness tester. Vibrating sample magnetometer (VSM, LAKESHORE-7304, USA) was used to characterize the magnetic properties of products.

The gel content of nanocomposites (W %) was carried out as follows: cleaning the film surface with ethanol, and then take two pieces of samples from the same film to identify the mass (M). Subsequently, the samples were immersed in acetone and kept rocking in shaker for 48 h, followed by extraction and weighted the samples mass (m) after drying in vacuum for 24 h. The gel content is the average of the two samples and is calculated as following formula:

$$W\% = \frac{m}{M} * 100\%$$

Water absorption and toluene resistance ability of nanocomposite films were tested according to GB/T1034-1998 by immersing a certain amount of films (M) in water or toluene, and weight the mass of the films (m) after a specified time. The water absorption and toluene absorption of nanocomposite films (W %) is calculated according to following formula:

$$W\% = \frac{m - M}{M} * 100\%$$

3. Results and discussion

3.1. Elemental analysis

Table 1 shows the data for elemental analysis of Fe_3O_4 and Fe_3O_4-VTEO. Because there was no nitrogen existing in both Fe_3O_4 and Fe_3O_4-VTEO, the nitrogen content was always zero. As depicted in Table 1, the carbon content and hydrogen content of Fe_3O_4-VTEO increased by about 2 times than pristine Fe_3O_4, which indicated that the Fe_3O_4 was successfully functionalized by VTEO.

3.2. Microstructure and morphology of Fe_3O_4 nanoparticles and nanocomposite films

Fig. 3 presents the TEM image of Fe_3O_4 particles. The Fe_3O_4 particles are spherical with diameters ranging from 200 to 300 nm. Fig. 4 shows the SEM micrographs of cross-section of the pure HWPU and HWPU/Fe_3O_4 nanocomposite films. Fig. 4a is the morphology of pure HWPU, the surface of HWPU is smooth. It is observed from Fig. 4b and c that the HWPU/Fe_3O_4 nanocomposites exhibit much rougher fractured surface than pure HWPU. HWPU/Fe_3O_4-0.5 and HWPU/Fe_3O_4-2 show better dispersion in HWPU matrix than HWPU/Fe_3O_4-6 (Fig. 4d). A large agglomeration occurred in HWPU/Fe_3O_4-6. Because with the increasing of Fe_3O_4-VTEO content in HWPU matrix, parts of Fe_3O_4-VTEO nanoparticles can't be wrapped in HWPU but exist in water phase, this would lead to large agglomeration of Fe_3O_4-VTEO particle itself. The uniform dispersion or agglomeration would have a great influence on thermal behavior and mechanical properties of film materials, [30] which we will discuss in detail below.

FT-IR was conducted to indentify the microstructure of Fe_3O_4-VTEO nanoparticles and HWPU/Fe_3O_4 nanocomposite. It is observed from Fig. 5a that the peaks at 3063 and 964 cm^{-1} are the stretching vibration and bending vibration absorption peaks of C-H from CH_2=C bonds, respectively. The characteristic stretching peaks of -CH_3 and -CH_2 occurred at 2959 and 2891 cm^{-1} in both Fig. 5a and b. The peaks at 1632 and 1411 cm^{-1} could be assigned to the stretching and bending vibration absorption peaks of C=C bonds. 1277 cm^{-1} is the stretching peak of C-Si, and the broad absorption peaks occurred at 1098 and 760 cm^{-1} are ascribed to the asymmetric and symmetric stretching vibration of Si-O-Si. Furthermore, the characteristic peak of Fe-O in Fe_3O_4 is detected at 570 cm^{-1}. Above analysis demonstrated that we have prepared Fe_3O_4-VTEO nanoparticles successfully, namely VTEO was successfully loaded on the magnetic Fe_3O_4 surface. Fig. 5b is the FT-IR spectrum of HWPU/Fe_3O_4-2. Absorption peaks at 3390 and 1533 cm^{-1} are the stretching and blending peaks of -N-H bonds of carbamate groups, respectively. The characteristic peak of C=O is observed at 1723 cm^{-1}. The absorption peaks at 2964 and 2885 cm^{-1} are assigned to -CH_3 and -CH_2. Moreover, compared with Fig. 5a, there are no obvious peaks at 1632 and 1411 cm^{-1} of C=C bonds, which implied that most of C=C double bonds in HWPU and Fe_3O_4-VTEO have participated in radical polymerization during the UV-curing process. The results proved that HWPU/Fe_3O_4 nanocomposite films have been successfully synthesized and the UV-curing was effective.

XRD patterns of Fe_3O_4-VTEO and HWPU/Fe_3O_4 nanocomposites are presented in Fig. 6. According to JCPDS 19-629 (JCPDS = Joint Committee on Powder

Diffraction Standards), the characteristic diffraction peaks of Fe_3O_4 at 2θ = 30°，36°，43°，53°，57° and 63° are clearly observed in both Fe_3O_4-VTEO (Fig. 6a) and HWPU/Fe_3O_4-4 (Fig. 6b), and the diffraction peaks of HWPU/Fe_3O_4 become weaker than Fe_3O_4-VTEO. The above analysis shows that the modification of Fe_3O_4 can't change the inverse spinel structure of Fe_3O_4 and the HWPU/Fe_3O_4 nanocomposites have been successfully synthesized. In addition, a new broad absorption peak between 15° and 30° occurred in HWPU/Fe_3O_4-4, which could be attributed to the orderly arrangement of soft segments in HWPU chains. [5, 31]

3.3. The properties characterization of HWPU/Fe_3O_4 nanocomposites

3.3.1 The stability of HWPU/Fe_3O_4 nanocomposites emulsion

The test for emulsion stability was conducted as follows: Keep the nanocomposite emulsion with different Fe_3O_4-VTEO content standing under natural condition and observe the storage stability of the emulsion. The test result is shown in Table 2. It was found that Fe_3O_4-VTEO content had a great effect on emulsion appearance and stability. The color of emulsion gradually deepened with the increasing of Fe_3O_4-VTEO content, and the emulsion with high Fe_3O_4-VTEO content exhibited poorer stability. The HWPU/Fe_3O_4-2 emulsion could place for about one month before delamination while less than 7 days for HWPU/Fe_3O_4-6 emulsion. In summary, parts of Fe_3O_4-VTEO nanoparticles were precipitated off gradually in a month, no matter how much the Fe_3O_4-VTEO content was. The reason might be that the HWPU combined with Fe_3O_4-VTEO nanoparticles by simple physical mixing rather than chemical interaction, or there was no strong interaction formed between them before

UV-curing process. Therefore, a part of Fe_3O_4-VTEO nanoparticles would be wrapped in HWPU in the mixing process, and also some nanoparticles would exist in water phase, which could cause agglomeration of Fe_3O_4-VTEO nanoparticles (especially in the system with high Fe_3O_4-VTEO content) and lead to poor stability of emulsion.

3.3.2. Gel content analysis of HWPU/Fe_3O_4 nanocomposites

The gel content of HWPU/Fe_3O_4 nanocomposites was performed to explore the effect of Fe_3O_4-VTEO content on cross-linking density of nanocomposites. It is observed from Fig. 7 that the gel content increases as the Fe_3O_4-VTEO content increase; this may be attributed to the improvement of cross-linking density. The C=C on Fe_3O_4-VTEO and HWPU chains can be cross-linked with each other in UV-curing process, which would contribute to the increase of cross-linking density. However, gel content begin to decrease when the Fe_3O_4-VTEO content reaches to more than 2%, this can be explained as: the more Fe_3O_4-VTEO content, the more agglomeration. Inorganic particles can't be dispersed homogeneously in HWPU matrix, parts of Fe_3O_4-VTEO would isolate out from polymer rather than cross-link, resulting in the decrease of gel content of nanocomposites.

3.3.3. Thermal properties of HWPU/Fe_3O_4 nanocomposites

To investigate the effect of Fe_3O_4 content on thermal stability of HWPU/Fe_3O_4 nanocomposites, TGA was conducted. Fig. 8 presents the typical TGA curves of pure HWPU and HWPU nanocomposites. It is observed that Fe_3O_4 fillers distinctly affected the thermal stability of nanocomposite films and all samples exhibited two weight loss stages. The thermal decomposition temperature range in first weight loss

stage is between 220 and 392 °C, is due to the decomposition of the hard segment of polymer. The second weight loss stage, from 392 to 490 °C, results from the decomposition of soft segments in the HWPU matrix. The Fe_3O_4 filler provides a higher initial degradation temperature for nanocomposites than pure WPU. The initial degradation temperature increases from 226 °C of HWPU to 252 °C of HWPU/Fe_3O_4-4, which is higher than the work we reported. [22] What's more, the thermal degradation rate decreases as Fe_3O_4 content increases, this indicates that the addition of Fe_3O_4 boost the thermal stability of the HWPU, and this can be explained as follows: The Fe_3O_4 inorganic oxide endows HWPU with high temperature stability. In addition, the functionalized Fe_3O_4 contains plenty of C=C double bonds, and would participate in radical polymerization in the UV-curing process, which could cause the improvement of crosslink density, thereby contributed to the thermal stability.

3.3.4. The dynamic thermal mechanical analysis of HWPU/Fe_3O_4 nanocomposites

The dynamic thermal mechanical analysis was measured to investigate the viscoelastic property of nanocomposites. The storage modulus (E′) and loss factor (tan δ) curves are shown in Fig. 9 and 10. The glass transition temperature (T_g) is obtained from the tan δ curve. E′ is relevant to cross-linking density and interfacial interaction. It is observed that both E′ and T_g increase as the Fe_3O_4-VTEO content increases, and revealed that the cross-linking density was improved. The T_g value increases from 115 °C of pure HWPU to 128 °C of HWPU/Fe_3O_4-2 and is higher than our previous work, [22] this may be attributed to the interaction between the organic and inorganic phases. [20] In addition, the introduction of Fe_3O_4-VTEO can enhance rigidity

of nanocomposites, therefore, the loss factor decreases and T_g value increases, which implied that the phases mixed evenly. However, due to agglomeration of Fe_3O_4-VTEO nanoparticle itself, E′ and T_g show a downward trend when the Fe_3O_4-VTEO content is more than 2%. There existed interaction in inorganic nanoparticles, nanoparticles would aggregate at high density, which can intensify the incompatibility of composite emulsion system and reduce cross-link of density in turn, resulting in the decrease of storage modulus and glass transition temperature. [32]

3.3.5. Water absorption and toluene absorption of nanocomposites

The influence of functionalized Fe_3O_4 content on water absorption and toluene absorption of nanocomposites are shown in Fig. 11 and 12. It is observed from Fig. 11 that the water absorption of nanocomposite decreases as the Fe_3O_4-VTEO increases, and without swelling observed. From the curves of 2%, 4% and 6%, the water absorption are 9%, 7% and 4% in 100 h, respectively, which are lower than 0.5% (13% in 100 h). This is attributed to the improvement of cross-linking density of HWPU/Fe_3O_4 system. What's more, the toluene absorption was also investigated and shown in Fig. 12. The toluene absorption of nanocomposites decreases with the increasing of Fe_3O_4-VTEO content, and toluene absorption of nanocomposites with Fe_3O_4-VTEO content of 2%, 4%, 6% are 8%, 4%, 2% in 120 h, respectively, which are lower than HWPU/Fe_3O_4-0.5% (22% in 120 h), the reason for this as above stated for water absorption. In summary, the increased Fe_3O_4-VTEO content contributed to better hydrophobicity of nanocomposites.

3.3.6. Mechanical properties of HWPU/Fe_3O_4 nanocomposites

The mechanical properties of pure HWPU and nanocomposites with different Fe_3O_4-VTEO content were investigated by tensile testing. The tensile strength, elongation at break and Young's modulus data of pure HWPU and nanocomposites are shown in Table 3. It is found that the mechanical properties of nanocomposites are largely affected by Fe_3O_4-VTEO nanoparticles. Compared with pure HWPU, the tensile strength, elongation at break and Young's modulus of nanocomposites gradually decrease with the increasing content of Fe_3O_4-VTEO. This can be explained as follows: the rigidity of nanocomposites was boosted with the introduction of Fe_3O_4-VTEO, moreover, the interaction between inorganic particles is stronger than the interaction between particles and polymer due to agglomeration of nanoparticles. This makes it difficult for Fe_3O_4-VTEO nanoparticles to disperse uniformly in polymer matrix in small size, which would lead to the phase separation and cause the decrease of tensile strength. Additionally, the hardness test of nanocomposites with different Fe_3O_4-VTEO loading is observed from Table 3. We can see that the hardness of the nanocomposites gradually strengthens as the Fe_3O_4-VTEO content increases. The hardness reaches the maximum when the Fe_3O_4-VTEO content is 2% and then decreased with the increasing of Fe_3O_4-VTEO content. Fe_3O_4-VTEO is rigid nanoparticle and can enhance stiffness of nanocomposites at the proper adding amount. Furthermore, the functionalized Fe_3O_4 acted as cross-linker and could make the nanocomposites further cross-linking, thereby increase the cross-link of density, which would also contribute to hardness of materials. However, if excessive Fe_3O_4-VTEO nanoparticles were added, the interaction between inorganic

nanoparticles will be stronger than the forces between inorganic and organic phases, this can cause agglomeration of nanoparticles and make the heterogeneous distribution of material inside, so the hardness of nanocomposites are obviously reduced.

3.3.7. Magnetic properties of HWPU/Fe_3O_4 nanocomposites

The magnetic properties of Fe_3O_4 and nanocomposites were characterized by vibrating sample magnetometer at room temperature. Fig. 13 shows the hysteresis loops of Fe_3O_4 and Fe_3O_4-VTEO. The maximum saturation magnetization (Ms) of Fe_3O_4 is 85.9 emu/g while reduces to 45.0 emu/g for Fe_3O_4-VTEO. The coercive force (Hc) and remnant magnetization (Mr) are almost zero. Therefore, both Fe_3O_4 and Fe_3O_4-VTEO present superior magnetic behavior and further proofed that the VTEO was successfully grafted on Fe_3O_4 surface. Fig. 14 shows the hysteresis loops of nanocomposites with different Fe_3O_4-VTEO content, it is observed that the nanocomposites possess good magnetic properties and the maximum saturation magnetization increases as the Fe_3O_4-VTEO content increases. The maximum saturation magnetization value reaches 12.20 emu/g with Fe_3O_4-VTEO content is 8%, which is higher than some reported works of film nanocomposites. [33-35] The magnetic properties are affected by nanoparticle size, surface disorder and distribution. [36] That is, the functionalization of Fe_3O_4 improved the distribution of nanoparticles in the nanocomposites compared the pristine nanoparticles, leading to the better magnetization of HWPU/Fe_3O_4 nanocomposites. The results revealed that the Fe_3O_4-VTEO has been combined successfully with HWPU and the nanocomposites

obtained magnetism from Fe_3O_4 fillers.

Conclusions

The HWPU/Fe_3O_4 nanocomposites were successfully synthesized by *in situ* polymerization method. The Fe_3O_4 was modified by chemical method and combined with HWPU through covalent bonds. The morphology of nanocomposites was characterized by SEM and suggested that Fe_3O_4-VTEO nanoparticles were wrapped and dispersed homogeneously in HWPU matrix at the low Fe_3O_4-VTEO content. It was found that the introduction of proper doping amount of Fe_3O_4-VTEO contributed to thermal stability, glass transition temperature, storage modulus, gel content, hardness and water, toluene resistance of nanocomposite films. The emulsion stability, tensile strength, Young's modulus and elongation at break decreased with the increasing of Fe_3O_4-VTEO content. Moreover, the resulting HWPU/Fe_3O_4 nanocomposites have exhibited better magnetic properties and would have a promising application in microwave - absorption field. Further investigation is now in progress.

Acknowledgements

The authors gratefully acknowledge financial supports from the National Training Fund for Talented Person of Basic Subjects ((J1103307) and the Opening Foundation of State Key Laboratory of Applied Organic Chemistry (SKLAOC-2009-35).

References

[1] S. Kango, S. Kalia, A. Celli, J. Njuguna, Y. Habibi, and R. Kumar, *Prog. Polym. Sci.*, 2013, **38**, 1232-1261.

[2] N. Nabih, K. Landfester and A. Taden, *J. Polym. Sci. Pol. Chem.*, 2011, **49**, 5019-5029.

[3] C. Xiao, Q. Wu, A. Chang, Y. Peng, W. Xu and W. Wu, *J., Mater. Chem. A.*, 2014.

[4] J. Zhang, X. Ge, M. Wang, J. Yang, Q. Wu, M. Wu and D. Xu, *Polym. Chem.*, 2011, **2**, 970-974.

[5] L. Wang, Y. Shen, X. Lai and Z. Li, J. *Appl. Polym. Sci.*, 2011, **119**, 3521-3530.

[6] Y. Heo, H. Im, J. Kim and J. Kim, *J. Nanopart. Res.*, 2012, **14**, 1-10.

[7] S. Srivastava and R. K. Tiwari, *Int. J. Polym. Mater.*, 2012, **61**, 999-1010.

[8] N. S. T. Do, D. M. Schaetzl, B. Dey, A. C. Seabaugh and S. K Fullerton-Shirey, *J. Phys. Chem. C.*, 2012, **116**, 21216-21223.

[9] O. Gencel, W. Brostow, G. Martinez-Barrera and M. S. Gok, Polimery., 2012, **57**, 276-283.

[10] K. W. Putz, O. C. Compton, M. J. Palmeri, S. T. Nguyen and L. C. Brinson, *And. Funct. Mater.*, 2010;, **20**, 3322-3329.

[11] Z. Spitalsky, D. Tasis, K. Papagelis and C. Galiotis, *Prog. Polym. Sci.*, 2010, **35**, 357-401.

[12] S. Y. Yang, W. N. Lin, Y. L. Huang, H. W. Tien, J. Y. Wang, C. C. M. Ma, ... and Y. S. Wang, *Carbon* 2011, **49**, 793-803.

[13] X. Wang, P. D. Bradford, W. Liu, H. Zhao, Y. Inoue, J. P. Maria, ... and Y. Zhu, *Compos. Sci. Technol.*, 2011, **71**, 1677-1683.

[14] K. Wongtimnoi, B. Guiffard, A. Bogner-Van De Moortele, L. Seveyrat, C. Gauthier and J. Y. Cavaillé, *Compos. Sci. Technol.*, 2011, **71**, 885-892.

[15] L. Peng, L. Zhou, Y. Li, F. Pan and S. Zhang, *Compos. Sci. Technol.*, 2011; **71**, 1280-1285.

[16] A. Bendahou, H. Kaddami, E. Espuche, F. Gouanvé and A. Dufresne, *Macromol. Mater. Eng.*, 2011, **296**, 760-769.

[17] J. A. Mbey, S. Hoppe and F. Thomas, *Carbohyd. Polym.*, 2012, **88**, 213-222.

[18] L. Yao, C. Wu, Z. Yang, W. Qiu, P. Cui and T. Xu, *J. Appl. Polym. Sci.*, 2012, **124**, E216-E224.

[19] Z. Dai, Z. Li, L. Li and G. Xu, *Polym. Advan. Technol.*, 2011, **22**, 1905-1911.

[20] L. Zhang, H. Zhang and J. Guo, *Ind. Eng. Chem. Res.*, 2012, **51**, 8434-8441.

[21] D. Molina, G. Griffini, M. Levi and S. Turri, Polym. *Advan. Technol.*, 2014.

[22] S. Zhang, Y. Li, L. Peng, Q. Li, S. Chen and K. Hou, *Compos. Part A-Appl. S.*, 2013, **55**, 94-101.

[23] S. H. Hsu, H. J. Tseng and Y. C. Lin, *Biomaterials.*, 2010, **31**, 6796-6808.

[24] B. Zhao, R. W. Fu, M. Q. Zhang, H. Yang, M. Z. Rong and Q. Zheng, *Polym. J.*, 2006, **38**, 799-806.

[25] C. Sow, B. Riedl and P. Blanchet, *J. Coat. Technol. Res.*, 2011, **8**, 211-221.

[26] S. Zhang, J. Jiang, C. Yang, M. Chen and X. Liu, *Prog. Org. Coat.*, 2011, **70**, 1-8.

[27] I. Rabias, M. Fardis, E. Devlin, N. Boukos, D. Tsitrouli and G. Papavassiliou, *ACS. Nano.*, 2008, **2**, 977-983.

[28] E. Açıkalın, O. Atıcı, A. Sayıntı, K. Çoban and H. Erkalfa, *Prog. Org. Coat.*, 2013, **76**, 972-978.

[29] A. H. Lu, E. E. Salabas and F. Schüth, *Angew. Chem. Int. Edit.*, 2007, **46**,

1222-1244.

[30] F. Yan, J. Li, J. Zhang, F. Liu and W. Yang, *J. Nanopart. Res.*, 2009, **11**, 289-296.

[31] L. Xiaojuan, L. Xiaorui, W. Lei and S. Yiding, *Polym. Bull.*, 2010, **65**, 45-57.

[32] C. M. Yakacki, N. S. Satarkar, K. Gall, R. Likos and J. Z. Hilt, *J. Appl. Polym. Sci.*, 2009, **112**, 3166-3176.

[33] M. Ashjari, A. R. Mahdavian, N. G. Ebrahimi and Y. Mosleh, *J. Magn. Magn. Mater.*, 2010, **20**, 213-219.

[34] I. Kong, S. Hj Ahmad, M. Hj Abdullah, D. Hui, A. Nazlim Yusoff and D. Puryanti, *J. Magn. Maga. Mater.*, 2010, **322**, 3401-3409.

[35] J. O. Park, K. Y. Rhee and S. J. Park, *Appl. Surf. Sci.*, 2010, **256**, 6945-6950.

[36] Z. Huang and F. Tang, *J. Colloid. In. Terf. Sci.*, 2004, **275**, 142-147.

Figure Captions:

Fig. 1. The reaction scheme of functional Fe_3O_4.

Fig. 2. The flowchart of the preparation of HWPU/Fe_3O_4 nanocomposite emulsion.

Fig. 3. TEM image of Fe_3O_4 nanoparticles.

Fig. 4. SEM micrographs of fractured section of pure HWPU (a), HWPU/Fe_3O_4-0.5 (b), HWPU/ Fe_3O_4-2 (c) and HWPU/ Fe_3O_4-6 .

Fig. 5. FT-IR spectra of Fe_3O_4-VTEO (a) and HWPU/Fe_3O_4-2 (b).

Fig. 6. XRD patterns of Fe_3O_4-VTEO (a) and HWPU/Fe_3O_4-4 (b).

Fig. 7. The gel content of nanocomposites with different Fe_3O_4-VTEO content.

Fig. 8. TGA curves of pure HWPU and HWPU/ Fe_3O_4 nanocomposites with different Fe_3O_4-VTEO content.

Fig. 9. DMA storage modulus curves of nanocomposites with different Fe_3O_4-VTEO content.

Fig. 10. DMA loss factor curves of nanocomposites with different Fe_3O_4-VTEO content.

Fig. 11. Influence of Fe_3O_4-VTEO content on water absorption of films.

Fig. 12. Influence of Fe_3O_4-VTEO content on toluene absorption of films.

Fig. 13. Hysteresis loops of Fe_3O_4 (a) and Fe_3O_4-VTEO (b).

Fig. 14. Hysteresis loops of HWPU/Fe_3O_4 nanocomposites with the Fe_3O_4-VTEO content is 8% (a), 4% (b) and 0.5% (c).

Table 1.

Elemental analysis of Fe_3O_4 and Fe_3O_4-VTEO.

Designation	N (%)	C (%)	H (%)
Fe_3O_4	0.00	2.53	0.41
Fe_3O_4-VTEO	0.00	4.62	0.66

Table 2.

The stability of HWPU/Fe_3O_4composite emulsion.

Fe_3O_4-VTEO content/%	0.5	1	2	4	6
emulsion stability	28 days	28 days	27 days	12 days	7 days
emulsion appearance	precipitation	precipitation	precipitation	precipitation	precipitation

Table 3.

The mechanical properties of HWPU and HWPU/Fe_3O_4 nanocomposites.

Designation	Pencil hardness	Tensile strength/MPa	Elongation at break (%)	Young's modulus/MPa
HWPU	2H	24.01	112.33	225.11
HWPU/Fe_3O_4-0.5	2H	16.98	100.76	164.67
HWPU/Fe_3O_4-2	2H	20.68	67.30	192.62
HWPU/Fe_3O_4-4	H	12.21	54.55	120.50
HWPU/Fe_3O_4-6	H	10.04	40.07	78.09